Zika virus cell tropism in the developing human brain and inhibition by azithromycin

Hanna Retallack[a,1], Elizabeth Di Lullo[b,c,1], Carolina Arias[a,d], Kristeene A. Knopp[a], Matthew T. Laurie[a], Carmen Sandoval-Espinosa[b,c], Walter R. Mancia Leon[b,c], Robert Krencik[e,f], Erik M. Ullian[e], Julien Spatazza[b,g], Alex A. Pollen[b,c], Caleigh Mandel-Brehm[a], Tomasz J. Nowakowski[b,c], Arnold R. Kriegstein[b,c,2], and Joseph L. DeRisi[a,2]

[a]Department of Biochemistry and Biophysics, University of California, San Francisco, CA 94158; [b]Eli and Edythe Broad Center of Regeneration Medicine and Stem Cell Research, University of California, San Francisco, CA 94143; [c]Department of Neurology, University of California, San Francisco, CA 94158; [d]Department of Molecular, Cellular, and Developmental Biology, University of California, Santa Barbara, CA 93106; [e]Department of Ophthalmology, University of California, San Francisco, CA 94122; [f]Center for Neuroregeneration, Department of Neurosurgery, Houston Methodist Research Institute, Houston, TX 77030; and [g]Department of Neurological Surgery, University of California, San Francisco, CA 94143

Contributed by Joseph L. DeRisi, November 1, 2016 (sent for review October 7, 2016; reviewed by Nenad Sestan and Pei-Yong Shi)

The rapid spread of Zika virus (ZIKV) and its association with abnormal brain development constitute a global health emergency. Congenital ZIKV infection produces a range of mild to severe pathologies, including microcephaly. To understand the pathophysiology of ZIKV infection, we used models of the developing brain that faithfully recapitulate the tissue architecture in early to midgestation. We identify the brain cell populations that are most susceptible to ZIKV infection in primary human tissue, provide evidence for a mechanism of viral entry, and show that a commonly used antibiotic protects cultured brain cells by reducing viral proliferation. In the brain, ZIKV preferentially infected neural stem cells, astrocytes, oligodendrocyte precursor cells, and microglia, whereas neurons were less susceptible to infection. These findings suggest mechanisms for microcephaly and other pathologic features of infants with congenital ZIKV infection that are not explained by neural stem cell infection alone, such as calcifications in the cortical plate. Furthermore, we find that blocking the glia-enriched putative viral entry receptor AXL reduced ZIKV infection of astrocytes in vitro, and genetic knockdown of AXL in a glial cell line nearly abolished infection. Finally, we evaluate 2,177 compounds, focusing on drugs safe in pregnancy. We show that the macrolide antibiotic azithromycin reduced viral proliferation and virus-induced cytopathic effects in glial cell lines and human astrocytes. Our characterization of infection in the developing human brain clarifies the pathogenesis of congenital ZIKV infection and provides the basis for investigating possible therapeutic strategies to safely alleviate or prevent the most severe consequences of the epidemic.

Zika virus | cortical development | azithromycin | microcephaly

A correlation between congenital exposure to the mosquito-borne and sexually transmitted Zika flavivirus (ZIKV) and the increased incidence of severe microcephaly suggests a causal relationship between ZIKV infection and neurodevelopmental abnormalities (1, 2). However, the mechanisms of infection and specifically which cell populations are vulnerable to ZIKV during the course of human brain development remain unclear. Major insights have been drawn from in vitro models of human brain development and primary mouse tissues. In the developing mouse brain, ZIKV has been shown to infect radial glia and neurons (3), whereas studies in human pluripotent stem cell (hPSC)-derived neural cells have highlighted widespread infection and apoptosis of neural progenitor cells (4, 5). Because these models do not fully recapitulate the developmental events and cell types present during human brain development, these results may not faithfully represent ZIKV-induced pathology in vivo.

During human brain development, radial glial cells, the neural stem cells, give rise to diverse types of neuronal and glial cells, including neurons, oligodendrocytes, and astrocytes, in a temporally controlled pattern. We reasoned that identifying cell types that are especially vulnerable to viral infection would facilitate studies of the viral life cycle, including entry mechanisms and host cell requirements. Building on studies that suggested that enriched expression of the candidate entry factor AXL could confer vulnerability to ZIKV entry (6–8), we used AXL expression levels to predict that radial glia, astrocytes, microglia, and endothelial cells would be particularly vulnerable to infection (9). A recent study highlighted the utility of ex vivo models using primary human tissue samples to analyze the consequences of ZIKV infection in the human prenatal brain (7). Here we further use primary tissue samples from distinct stages of brain development corresponding to periods of peak neurogenesis and early gliogenesis.

Determining the tropism of ZIKV for specific cell types will help identify suitable cellular models for investigating potential therapeutic interventions. Although development of a vaccine could provide a long-term solution to the current ZIKV epidemic, there remains an unmet clinical need to identify drugs that can limit or prevent the consequences of congenital infection. A recent screen of a subset of Food and Drug Administration (FDA)-approved compounds against ZIKV in hepatic cells identified several anticancer, antimicrobial, antiparasitic, and antifungal drugs with anti-ZIKV activity (10). Another screen, based on human neural progenitor cells, identified an antifungal drug and

Significance

Zika virus (ZIKV) is a mosquito-borne flavivirus that has rapidly spread through the Americas and has been associated with fetal abnormalities, including microcephaly. To understand how microcephaly develops, it is important to identify which cell types of the developing brain are susceptible to infection. We use primary human tissue to show that radial glia and astrocytes are more susceptible to infection than neurons, a pattern that correlates with expression of a putative viral entry receptor, AXL. We also perform a screen of Food and Drug Administration-approved compounds, with an emphasis on drugs known to be safe in pregnancy. We identify an antibiotic, azithromycin, that reduces viral proliferation in glial cells, and compare its activity with daptomycin and sofosbuvir, two additional drugs with anti-ZIKV activity.

Author contributions: H.R., E.D.L., C.A., K.A.K., M.T.L., A.A.P., T.J.N., A.R.K., and J.L.D. designed research; H.R., E.D.L., C.A., K.A.K., M.T.L., C.S.-E., W.R.M.L., J.S., and C.M.-B. performed research; R.K. and E.M.U. contributed new reagents/analytic tools; H.R., E.D.L., C.A., K.A.K., M.T.L., C.S.-E., W.R.M.L., J.S., C.M.-B., and T.J.N. analyzed data; and H.R., E.D.L., C.A., K.A.K., M.T.L., A.A.P., T.J.N., A.R.K., and J.L.D. wrote the paper.

Reviewers: N.S., Yale University School of Medicine; and P.-Y.S., University of Texas Medical Branch.

The authors declare no conflict of interest.

Freely available online through the PNAS open access option.

[1]H.R. and E.D.L. contributed equally to this work.

[2]To whom correspondence may be addressed. Email: kriegsteina@stemcell.ucsf.edu or joe@derisilab.ucsf.edu.

This article contains supporting information online at www.pnas.org/lookup/suppl/doi:10.1073/pnas.1618029113/-/DCSupplemental.

several scaffold compounds for further development (11). However, the majority of compounds with anti-ZIKV activity from these screens are contraindicated or of unknown safety during pregnancy. Furthermore, two promising candidates that might be safe during pregnancy, daptomycin and sofosbuvir, showed variable effectiveness by cell type (7, 10, 12). Combining unbiased screens of approved compounds with comparisons of top candidates with known antiviral activity may quickly narrow the search for drugs that could mitigate the effects of congenital ZIKV infection.

Here we assessed ZIKV cell tropism in the developing human brain and performed a drug screen on relevant cell types targeted by the virus with an emphasis on drugs known to be safe in pregnancy. We found that radial glia and, later in development, astrocytes were especially vulnerable to ZIKV infection. By screening FDA-approved

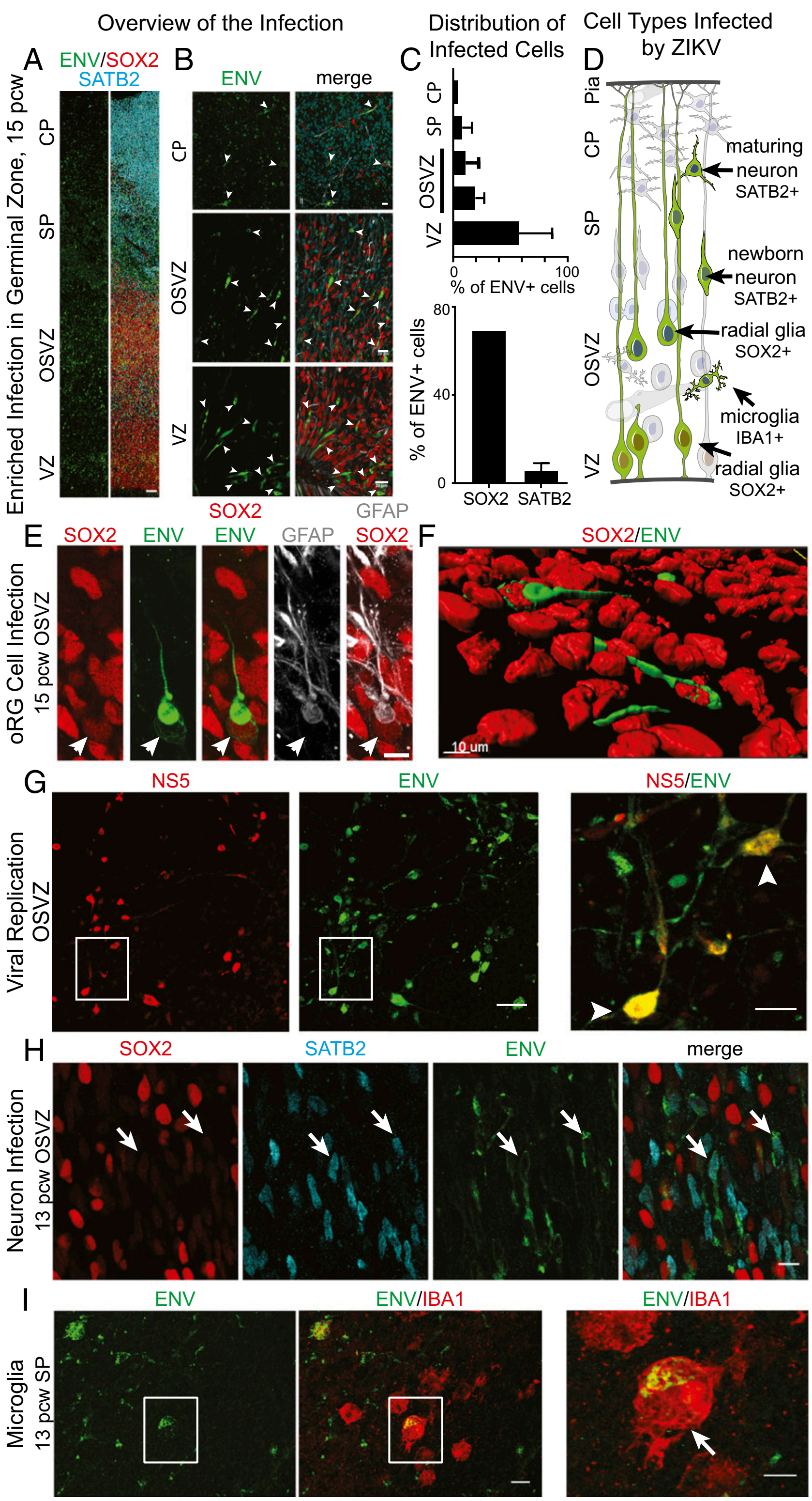

Fig. 1. Tropism of ZIKV for radial glia in the developing human brain. Human cortical organotypic brain slices were infected with ZIKV-BR and cultured for 72 h. (*A* and *B*) Low-magnification overview of ZIKV infection detected by ENV (green) within the cortex. (*A*) ENV staining was analyzed with respect to region and cell type. CP, cortical plate; OSVZ, outer subventricular zone; SP, subplate; VZ, ventricular zone. (Scale bar, 100 μm.) (*B*) High magnification of *A*. Notably, ENV staining (arrowheads) appears to be preferentially enriched in the VZ and OSVZ. (Scale bars, 20 μM.) (*C*) Quantification of ENV^{+} cells by region (*Top*) and cell type (*Bottom*) at 13 to 14 pcw. $n = 2$; mean ± SD [*SI Materials and Methods*; an error bar is not shown where it is shorter than the line thickness (*Top*, CP; *Bottom*, SOX2)]. (*D*) Schematic summary of cell types observed to be susceptible to ZIKV infection (green) in the developing human brain during midneurogenesis. (*E*) High-magnification view of a ZIKV-infected radial glial cell in the OSVZ (arrow). oRG, outer radial glial. (Scale bar, 10 μm.) (*F*) Three-dimensional reconstruction of *E*, highlighting the intracellular presence of the ENV signal. (Scale bar, 10 μm.) (*G*) ENV and NS5 signal in OSVZ cells (arrowheads) suggested replicating ZIKV-PR. (Scale bars, 20 μm.) (*H*) Immature neurons (SATB2^{+}, blue) infected with ZIKV (arrows). (Scale bar, 20 μm.) (*I*) Microglia (IBA1^{+}) immunopositive for ENV. High magnification (*Right*) shows ENV^{+} microglia with amoeboid morphology (arrow), typical of activated microglia. (Scale bars, 10 μm.)

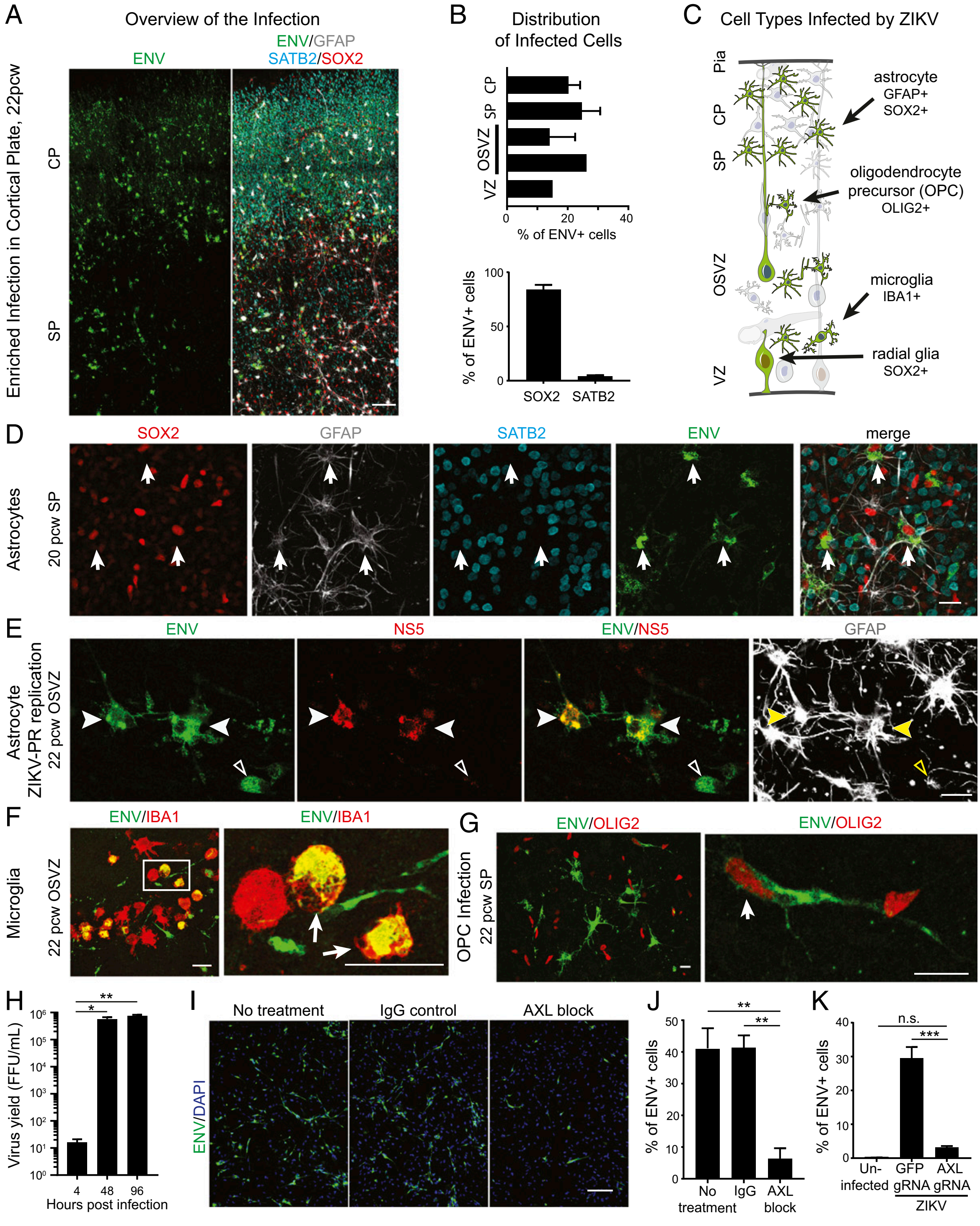

Fig. 2. ZIKV infects astrocytes in later stages of human brain development. (*A*) Low-magnification overview of ZIKV infection detected by ENV (green) within human organotypic cortical slices during late neurogenesis/gliogenesis. (Scale bar, 100 μm.) (*B*) Quantification of ENV$^+$ cells by region (*Top*) and cell type (*Bottom*) at 20 to 22 pcw. $n = 2$; mean ± SD [*SI Materials and Methods*; an error bar is not shown where shorter than the line thickness (*Top*, VZ and second OSVZ)]. (*C*) Schematic summary of cell types observed to be susceptible to ZIKV infection (green). (*D* and *E*) Immunohistochemical analysis reveals ZIKV infection in astrocytes by positivity for ENV (arrows, *D*; arrowheads, E) or ENV and nonstructural protein NS5, indicating active viral replication (filled arrowheads, *E*). (Scale bars, 20 μm.) (*F*) Microglia colabeled with ENV (arrows). (Scale bars, 50 μm.) (*G*) ZIKV infection of oligodendrocyte precursor cells (OPCs, arrow). (Scale bars, 20 μm.) (*H*) Viral production in 19-pcw cortical slices, quantified by focus-forming assay from combined homogenized tissue and conditioned media at 4, 48, and 96 h postinfection. FFU, focus-forming units. Two independent biological replicates with two technical replicates for each time point; mean ± SEM; one-way ANOVA with Tukey's multiple comparisons test, $*P \leq 0.05$, $**P \leq 0.01$; see also Fig. S4*F*. (*I* and *J*) Analysis of ZIKV-BR infection in the presence of AXL-blocking antibody in hPSC-derived astrocytes (*SI Materials and Methods*). Note the reduced ENV staining with AXL block compared with IgG control. (Scale bar, 100 μm.) (*J*) Quantification of the experiment represented in *I*; see also Fig. S5*A*; $n = 3$; mean ± SEM; one-way ANOVA with Tukey's multiple comparisons test, $**P \leq 0.01$. (*K*) ZIKV-PR infection after knockdown of AXL using U87-dCas9 lines expressing either GFP guide (g)RNA (nontargeting control) or AXL gRNAs (dCas9-mediated knockdown); see also Fig. S5*B*; two biological replicates in cell lines generated with independent transductions; mean ± SEM; two-way ANOVA with Tukey's multiple comparisons test, n.s. (not significant), $***P \leq 0.001$.

compounds for anti-ZIKV activity in a glial cell line with features of both cell types, we also found that the common antibiotic azithromycin prevented viral production and virus-mediated cell death, which we further validated in human astrocytes.

Results

To determine the cell populations most susceptible to ZIKV infection, we investigated the infectivity of ZIKV in the developing human brain using organotypic cultures from primary human tissue. We exposed human cortical tissue slices to three strains of ZIKV: Cambodia 2010 (ZIKV-CAM), Brazil 2015 (ZIKV-BR), and Puerto Rico 2015 (ZIKV-PR), cultured them for 72 h, and detected infection by immunostaining for the flavivirus envelope protein (ENV), an approach we validated in cultured cells (Fig. S1). Infection in tissue was confirmed by immunostaining for the viral RNA-dependent RNA polymerase nonstructural protein 5 (NS5), present only during viral replication. In samples from midneurogenesis [13 to 16 postconception wk (pcw)], we observed high rates of infection in the ventricular and subventricular zones (Fig. 1 and Fig. S2). We found that the virus preferentially infected both ventricular and outer radial glial cells (Fig. 1 *A–F* and Fig. S2). Interestingly, we observed clusters of infected radial glia (Fig. S2*B*), which may reflect local viral spread. A minor fraction of cells positive for ENV at these stages included postmitotic neurons (Fig. 1*H*) and microglia (Fig. 1*I*). We observed similar patterns of infection across ZIKV strains (Fig. S2). We also observed a small but significant increase in cell death of ENV$^+$ cells compared with ENV$^-$ cells in ZIKV-infected or mock-infected tissue (Fig. S3).

At later stages of development (after 17 pcw), we observed infection and viral replication throughout the developing cortex, including the cortical plate and subplate, with production of infectious virus by 48 h postinfection (hpi) (Fig. 2 and Fig. S4). Among cortical plate cells, we observed a high rate of infection in astrocytes, as distinguished by their location, morphology, and immunoreactivity with the glial markers GFAP and SOX2 (Fig. 2 *A*, *B*, and *D* and Fig. S4 *A–D*). We also observed cells immunoreactive for both ENV and the microglial marker IBA1, indicating microglial infection or phagocytosis of other ZIKV-infected cells (Fig. 2*F* and Fig. S4 *G* and *H*). This ENV$^+$/IBA1$^+$ microglial population was quantified at $7 \pm 1\%$ of ENV$^+$ cells, and represented $7 \pm 2\%$ of the total IBA1$^+$ population (n = 4, 15 to 22 pcw; *SI Materials and Methods*). We further observed infection of oligodendrocyte precursor cells (Fig. 2*G* and Fig. S4*I*) but limited infection of neurons (Fig. 2 *B* and *D* and Fig. S4 *A* and *J*). This pattern of infectivity was consistent across ZIKV strains (Fig. S4), and matched viral tropism predicted by AXL receptor expression (9).

To test the possible role of AXL in mediating ZIKV entry into human astrocytes, we infected hPSC-derived astrocytes (13, 14) in the presence of a nonactivating antibody specific for the extracellular domain of AXL. Blocking the AXL receptor substantially reduced infection (Fig. 2 *I* and *J* and Fig. S5*A*). To further test the requirement of AXL for ZIKV infection of glial cells, we used the U87 glioblastoma line that expresses high levels of astrocyte marker genes and AXL (15). U87 cells were readily infected with ZIKV, with strong virus production at 48 hpi (Fig. S1) and robust cytopathic effect at 72 hpi (Fig. 3*C* and Fig. S6*D*). We then used CRISPR interference (CRISPRi) to knock down AXL in this cell line (*SI Materials and Methods*; validated by Western blot in Fig. S5*B*) and observed a substantial decrease in infection (Fig. 2*K*), confirming the importance of this receptor for ZIKV infection in this cell type. Given that AXL is a receptor tyrosine kinase with signaling pathways that could be involved in innate immune responses (16), we tested whether the kinase activity of AXL was relevant for the decrease in infection observed in the knockdown line. After pretreatment with a small-molecule inhibitor, R428, we observed no decrease in infection at up to 1 μM, which is >70-fold the half-maximal effective concentration (EC_{50}) for AXL kinase inhibition (Fig. S5*C*) (17). Although we did observe a decrease in infection at 3 μM R428, this high concentration of >200-fold the EC_{50} likely created off-target effects. Together, these results suggest that AXL has an important role in glial cell infection that

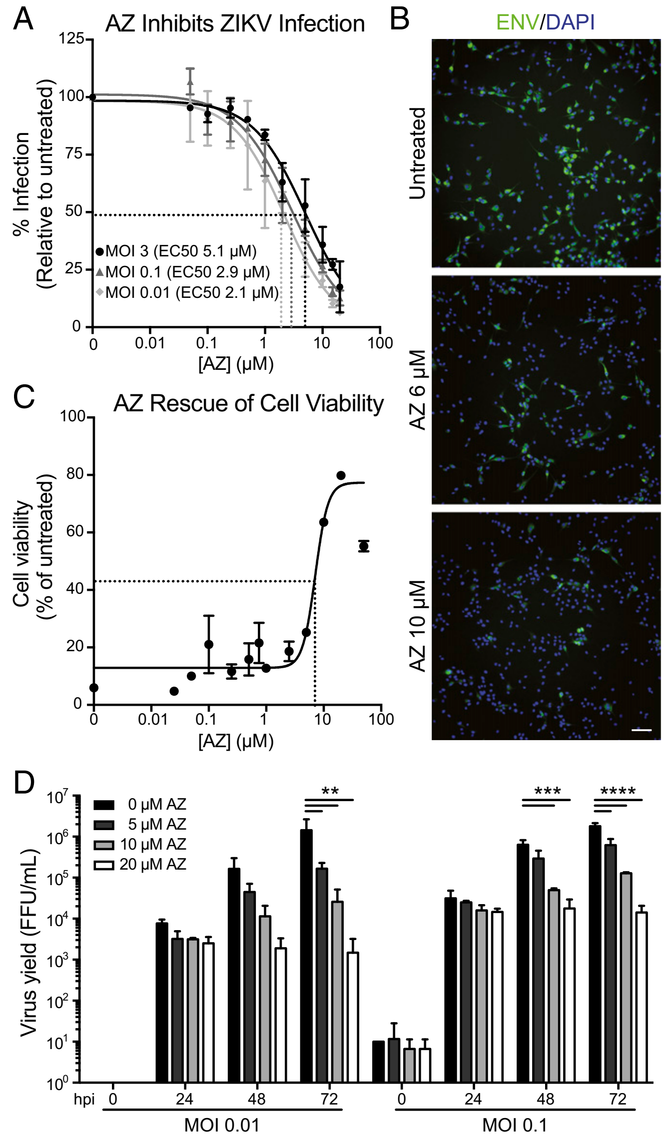

Fig. 3. Azithromycin treatment inhibits ZIKV infection in glial cells. (*A*) U87 cells were treated with increasing concentrations of AZ and infected with ZIKV-PR at varying MOIs (0.01, 0.1, and 3, as indicated). The percentage of infected cells at 48 hpi was determined by flow cytometry of cells immunostained for ENV and normalized to untreated cells (for raw data, see Fig. S6*A*). EC_{50} values for AZ-mediated reduction of ZIKV infection were 5.1 μM for an MOI of 3 (n = 2), 2.9 μM for an MOI of 0.1 (n = 2), and 2.1 μM for an MOI of 0.01 (n = 2); mean ± SD. (*B*) Representative images of U87 cells treated with AZ and infected with ZIKV-PR at an MOI of 3 (as in *A*). At 48 hpi, cells were immunostained for ENV protein (green) and cellular DNA (DAPI, blue). (Scale bar, 100 μm.) (*C*) Rescue of cell viability with AZ. U87 cells were pretreated with AZ for 1 h and then infected with ZIKV-PR at an MOI of 10 in the presence of AZ. Cell viability was measured at 72 hpi using the CellTiter-Glo luminescence assay. The EC_{50} value for the AZ-mediated rescue of cell viability was 7.1 μM. The data point at the highest concentration of AZ (50 μM) showed reduced cell viability, likely due to drug toxicity (Fig. S6*C*). n = 2; mean ± SD. (*D*) Decrease of virus production with AZ treatment. U87 cells were pretreated with AZ for 1 h and then infected with ZIKV-PR at an MOI of 0.1 or 0.01 in the presence of AZ. Quantification of virus yield in conditioned media was performed by focus-forming assay at 0, 24, 48, and 72 hpi; n = 2 for each MOI; mean ± SD; two-way ANOVA with Tukey's multiple comparisons testing, $^{**}P \leq 0.01$, $^{***}P \leq 0.001$, $^{****}P \leq 0.0001$.

depends more on its extracellular domain than on its intracellular kinase activity.

There is a pressing need to identify pharmacological compounds that can diminish the effects of ZIKV infection in relevant human cell types. We performed a screen of 2,177 clinically approved compounds (2,016 unique) by monitoring inhibition of virus-dependent cell death at 72 hpi in Vero cells. Although our screen revealed compounds that rescued cell viability, including antibiotics and inhibitors of nucleotide and protein synthesis, many showed toxicity in Vero or U87 cells or are contraindicated during pregnancy (Tables S1–S4). We focused on further characterization of the macrolide antibiotic azithromycin (AZ), which rescued ZIKV-induced cytopathic effect with low toxicity in our primary screens and is generally safe during pregnancy (18). AZ dramatically reduced ZIKV infection of U87 cells at an EC_{50} of 2 to 3 μM at multiplicities of infection (MOIs) of 0.01 to 0.1, as evaluated by ENV staining (Fig. 3 *A* and *B* and Fig. S6*A*). We further established a relationship between EC_{50} and baseline infection rate (Fig. S6*B*) and showed that even at >60% infection, AZ consistently reduced infection at concentrations 10- to 20-fold below the half-maximal toxicity concentration (TC_{50}) of 53 μM (Fig. S6 *A* and *C*). AZ treatment also rescued cell viability (Fig. 3*C* and Fig. S6*D*) and decreased viral production (Fig. 3*D*). Finally, we found that AZ substantially reduced infection in hPSC-derived astrocytes without toxicity at the effective concentration (EC_{50} 15 μM at 72% baseline infection) (Fig. S6 *E*–*G*). To compare AZ with compounds identified in previous screens, we evaluated the anti-ZIKV activity of daptomycin and sofosbuvir in U87 cells (EC_{50} 2.2 and 12.4 μM, respectively) (Fig. S6*H*). We observed that treatment with daptomycin was insufficient to lower the percentage of infected cells below 46% even at the highest dose in this cell type (20 μM) (Fig. S6*H*), whereas AZ and sofosbuvir treatment decreased ZIKV infection from 78 to below 5% infection at 20 and 50 μM, respectively. These results highlight AZ as a potential tool compound against ZIKV infection in glial cells.

Discussion

The rapid spread of ZIKV and its link to fetal abnormalities, including microcephaly, have created a global health crisis. Understanding viral tropism for specific cell types in the developing brain furthers our understanding of the pathophysiology of ZIKV-associated microcephaly and provides a basis for investigating antiviral drugs in a relevant cell type. Our findings offer several novel aspects. In particular, we show ZIKV tropism for astrocytes in addition to radial glia in the primary developing human brain, demonstrate the importance of AXL for ZIKV infection of glial cells, and identify a common antibiotic with anti-ZIKV activity, AZ, which we compare with two other drugs with anti-ZIKV activity that may be safe in pregnancy.

Our finding that radial glia are preferentially infected during early neurogenesis is consistent with experiments in cultured primary human brain cells (19), developing mouse cortex (3, 20), and primary human organotypic brain slice culture (7). These studies also reported overall survival of infected radial glia, in contrast to in vitro derived neural stem cells that undergo apoptotic cell death following infection (4, 5, 21). Cell lines derived from primary neural progenitors have variably shown infection with substantial apoptosis (7) or persistence (19). In our organotypic slice culture, we observe a small increase in apoptosis of infected cells. The discrepancy in levels of apoptosis in dissociated versus tissue cell culture may reflect differences in gene expression, maturation, or experimental conditions. Besides causing cell death, ZIKV infection could also affect cell-cycle progression (3, 21), differentiation, or the migration and survival of newborn neurons—mechanisms thought to underlie genetic causes of microcephaly and lissencephaly (22). Tissue disorganization in organotypic slice culture suggests these non–cell death-mediated mechanisms may contribute to clinical phenotypes (7), but this remains to be confirmed by directly analyzing cell behavior.

The high rate of infection in astrocytes at later developmental ages, many of which contact microcapillaries, could link our understanding of initial infection with clinical findings of cortical plate damage. For example, after prolonged infection, viral production in astrocytes could lead to a higher viral load in the cortical plate, causing infection of additional cortical cell types, and astrocyte loss could lead to inflammation and further damage, even in uninfected cells. Widespread cell death in vivo, which may take days to weeks to occur and is therefore outside the time frame of our experimental paradigm, is expected, given clinical reports of band-like calcifications in the cortical plate, cortical thinning, and hydrocephalus (2, 23). On the basis of their susceptibility to ZIKV infection and a central role in brain tissue homeostasis, human astrocytes provide a good cellular model for further investigation of mechanisms of viral entry and a platform for testing the efficacy of candidate therapeutic compounds.

Our observation that blocking or knocking down the AXL receptor prevents infection of human astrocytes, but that blocking intracellular kinase activity does not, suggests that the extracellular domain of AXL contributes to ZIKV infection whereas AXL signaling is dispensable. This extends comparable findings in endothelial cells to a cell type relevant for understanding microcephaly (6, 8) but does not address other viral receptors that may be important for ZIKV infectivity in other cell types or rule out a role for AXL signaling in the context of a full immune response in vivo. Although AXL knockout mice can be readily infected with ZIKV, disruption of the blood–brain barrier in these mice could lead to atypical routes for infection of the brain (24).

In addition to characterizing brain cell tropism, we also sought to identify possible therapeutic candidates with known safety profiles, especially in pregnancy. Several compounds expected to inhibit ZIKV were identified by our drug screen. These positive controls include the protein synthesis inhibitor cycloheximide, nucleic acid synthesis inhibitors such as mycophenolate derivatives, and intercalating compounds such as doxorubicin and homidium bromide. We additionally identified compounds that are known to be safe in pregnancy, including AZ. AZ is recommended for the treatment of pregnant women with sexually transmitted infections or respiratory infections due to AZ-susceptible bacteria (25, 26). Adverse events have not been observed in animal reproduction studies, and studies in pregnant women show no negative effects on pregnancy outcome or fetal health associated with AZ (18, 27). Orally administered AZ has been shown to reach concentrations of ~2.8 μM in the placenta, and is rapidly transported to amniotic fluid and umbilical cord plasma in humans (28, 29). Moreover, AZ accumulates in fetal tissue and in the adult human brain at concentrations from 4 to 21 μM (30, 31). Together, these pharmacokinetic studies suggest that AZ could rapidly accumulate in fetal tissue, including the placenta in vivo, at concentrations comparable to those that inhibit ZIKV proliferation in culture. Nonetheless, it remains unknown whether these in vitro results would be recapitulated in humans.

We further compared AZ with two promising drug candidates that might be safe in pregnancy and have reported anti-ZIKV activity in cell culture: daptomycin and sofosbuvir. Our dose–response curves are in agreement with the documented activity of sofosbuvir in human neuroepithelial stem cells (7), and extend the activity of daptomycin previously seen in HuH-7 and HeLa cells (10) to glial cells. We noted that daptomycin would not have been highly ranked in our initial screen due to the limited maximum effect of the drug as observed in dose–response curves. Unlike sofosbuvir, which likely targets the ZIKV RNA-dependent RNA polymerase (NS5) based on its mechanism against hepatitis C virus, daptomycin and AZ have unknown mechanisms of action against ZIKV. Nonetheless, the difference in in vitro dose–response between AZ and daptomycin is intriguing, and suggests different mechanisms of inhibition. Another important factor for a drug candidate for ZIKV treatment is accessibility. Access to sofosbuvir and its derivatives may be limited by its current price whereas AZ and daptomycin are available as generic forms, although daptomycin is not available in oral formulation due to poor oral bioavailability. Our comparison adds new data to consider alongside other antiviral activity data, safety, cost, and accessibility in moving forward with further exploration of these and related compounds. In parallel with direct comparisons in vitro, follow-up studies in animal models can be useful for prioritizing candidates. However, as with in vitro studies, there are caveats in interpreting animal models, such as substantial differences between human and mouse immune systems, placental structure, and fetal brain development.

Together, our work identifies cell type-specific patterns of ZIKV infection in second-trimester human developing brain, provides experimental evidence that AXL is important for ZIKV infection of relevant human brain cell types, and highlights a common antibiotic with inhibitory activity against ZIKV in glial cells. Ongoing studies will be required to determine whether AZ, daptomycin, sofosbuvir, and other inhibitors or combinations are capable of reducing ZIKV infection in the critical cell types identified here in vivo. Although preventative measures such as mosquito abatement and a ZIKV vaccine are imperative for long-term control of this pathogen, the study of ZIKV infection of primary human tissues and identification of inhibitors with therapeutic potential remain important components of a global response to this emerging threat.

Materials and Methods

Detailed materials and methods are available in *SI Materials and Methods*.

Cells and Viruses. Cell lines were Vero cells, U87 cells, and human astrocytes derived from human pluripotent stem cells (13). ZIKV strains were SPH2015 (Brazil 2015; ZIKV-BR), PRVABC59 (Puerto Rico 2015; ZIKV-PR), and FSS13025 (Cambodia 2010; ZIKV-CAM).

Brain Samples. Deidentified primary tissue samples were collected with previous patient consent in strict observance of the legal and institutional ethical regulations. Protocols were approved by the Human Gamete, Embryo and Stem Cell Research Committee (institutional review board) at the University of California, San Francisco (UCSF). Slices in organotypic culture were inoculated with ZIKV or mock-infected, fixed at 72 hpi or 5 d postinfection, and processed for immunohistochemistry. Quantification was performed on 13- to 22-pcw slices.

AXL. For 1 h before infection, cells were treated with AXL-blocking antibody or goat IgG control at 100 μg/mL, or with 1 to 3 μM R428 or vehicle (<0.1% DMSO). For AXL knockdown, U87 cells stably expressing dCas9-KRAB (15) were transduced with lentiviral particles expressing a pool of gRNAs targeting AXL or a gRNA targeting GFP as a control.

Drug Screen. A collection of 2,177 FDA-approved compounds, provided by the UCSF Small Molecule Discovery Center, was tested at 2 μM in Vero cells infected with ZIKV-BR (MOIs of 1, 3, and 10) and in U87 cells (MOI of 3). Toxicity screens in uninfected cells were performed in parallel. Cells were pretreated for 2 h before addition of ZIKV-BR or media, and cell viability was assessed at 72 hpi using the CellTiter-Glo 2.0 assay (Promega). Candidates with cell viability >2.5-fold that of untreated cells in every Vero cell screen were identified for follow-up.

Drug Validation. U87 cells or hPSC-derived astrocytes were treated with azithromycin, daptomycin, sofosbuvir, or vehicle for >1 h, and then infected with ZIKV-PR. Cell-viability assays were performed using CellTiter-Glo as above. To assess viral envelope production, cells were fixed and stained at 48 hpi using anti-flavivirus envelope protein, and then quantified by plate imaging with automated cell counting or by flow cytometry.

ACKNOWLEDGMENTS. We thank Marc and Lynne Benioff for their financial support of these studies. We also thank Susan Fisher (UCSF), Robert Tesh (UTMB), Nikos Vasilakis (UTMB), Julio Rodriguez-Andres (CSIRO), Graham Simmons (BSRI), Charles Chiu (UCSF), Dan Lim (UCSF), John Liu (UCSF), Max Horlbeck (UCSF), Shaohui Wang (UCSF), Diego Acosta-Alvear (UCSF), and the Small Molecule Discovery Center at UCSF for providing reagents and advice. This work was supported by NIH/NINDS Grants R01NS075998 and U01 MH105989 as well as a gift from Bernard Osher (to A.R.K.), Howard Hughes Medical Institute (J.L.D.), NIMH Grant R01MH099595-01 and Paul G. Allen Family Foundation Distinguished Investigator Award (to E.M.U.), and Damon Runyon Cancer Research Foundation Postdoctoral Fellowship DRG-2166-13 (to A.A.P.).

1. Brasil P, et al. (March 4, 2016) Zika virus infection in pregnant women in Rio de Janeiro—Preliminary report. *N Engl J Med*, 10.1056/NEJMoa1602412.
2. Mlakar J, et al. (2016) Zika virus associated with microcephaly. *N Engl J Med* 374(10):951–958.
3. Li C, et al. (2016) Zika virus disrupts neural progenitor development and leads to microcephaly in mice. *Cell Stem Cell* 19(1):120–126.
4. Tang H, et al. (2016) Zika virus infects human cortical neural progenitors and attenuates their growth. *Cell Stem Cell* 18(5):587–590.
5. Qian X, et al. (2016) Brain-region-specific organoids using mini-bioreactors for modeling ZIKV exposure. *Cell* 165(5):1238–1254.
6. Hamel R, et al. (2015) Biology of Zika virus infection in human skin cells. *J Virol* 89(17): 8880–8896.
7. Onorati M, et al. (2016) Zika virus disrupts phospho-TBK1 localization and mitosis in human neuroepithelial stem cells and radial glia. *Cell Reports* 16(10):2576–2592.
8. Liu S, DeLalio LJ, Isakson BE, Wang TT (September 20, 2016) AXL-mediated productive infection of human endothelial cells by Zika virus. *Circ Res*, 10.1161/CIRCRESAHA.116.309866.
9. Nowakowski TJ, et al. (2016) Expression analysis highlights AXL as a candidate Zika virus entry receptor in neural stem cells. *Cell Stem Cell* 18(5):591–596.
10. Barrows NJ, et al. (2016) A screen of FDA-approved drugs for inhibitors of Zika virus infection. *Cell Host Microbe* 20(2):259–270.
11. Xu M, et al. (2016) Identification of small-molecule inhibitors of Zika virus infection and induced neural cell death via a drug repurposing screen. *Nat Med* 22(10):1101–1107.
12. Sacramento CQ, et al. (2016) The clinically approved antiviral drug sofosbuvir impairs Brazilian Zika virus replication. bioRxiv. Available at biorxiv.org/content/early/2016/07/06/061671.
13. Krencik R, et al. (2015) Dysregulation of astrocyte extracellular signaling in Costello syndrome. *Sci Transl Med* 7(286):286ra66.
14. Krencik R, Weick JP, Liu Y, Zhang Z-J, Zhang S-C (2011) Specification of transplantable astroglial subtypes from human pluripotent stem cells. *Nat Biotechnol* 29(6):528–534.
15. Liu SJ, et al. (2016) Single-cell analysis of long non-coding RNAs in the developing human neocortex. *Genome Biol* 17:67.
16. Rothlin CV, Ghosh S, Zuniga EI, Oldstone MBA, Lemke G (2007) TAM receptors are pleiotropic inhibitors of the innate immune response. *Cell* 131(6):1124–1136.
17. Holland SJ, et al. (2010) R428, a selective small molecule inhibitor of Axl kinase, blocks tumor spread and prolongs survival in models of metastatic breast cancer. *Cancer Res* 70(4):1544–1554.
18. Lin KJ, Mitchell AA, Yau W-P, Louik C, Hernández-Díaz S (2013) Safety of macrolides during pregnancy. *Am J Obstet Gynecol* 208(3):221.e1–221.e8.
19. Hanners NW, et al. (2016) Western Zika virus in human fetal neural progenitors persists long term with partial cytopathic and limited immunogenic effects. *Cell Reports* 15(11):2315–2322.
20. Brault JB, et al. (2016) Comparative analysis between flaviviruses reveals specific neural stem cell tropism for Zika virus in the mouse developing neocortex. *EBioMedicine* 10:71–76.
21. Cugola FR, et al. (2016) The Brazilian Zika virus strain causes birth defects in experimental models. *Nature* 534(7606):267–271.
22. Thornton GK, Woods CG (2009) Primary microcephaly: Do all roads lead to Rome? *Trends Genet* 25(11):501–510.
23. Hazin AN, et al.; Microcephaly Epidemic Research Group (2016) Computed tomographic findings in microcephaly associated with Zika virus. *N Engl J Med* 374(22): 2193–2195.
24. Miner JJ, et al. (2016) Zika virus infection in mice causes panuveitis with shedding of virus in tears. *Cell Reports* 16(12):3208–3218.
25. Workowski KA, Bolan GA; Centers for Disease Control and Prevention (2015) Sexually transmitted diseases treatment guidelines, 2015. *MMWR Recomm Rep* 64(RR-03):1–137.
26. DHHS Panel on Opportunistic Infections in HIV-Infected Adults and Adolescents (2016) *Guidelines for the Prevention and Treatment of Opportunistic Infections in HIV-Infected Adults and Adolescents: Recommendations from the Centers for Disease Control and Prevention, the National Institutes of Health, and the HIV Medicine Association of the Infectious Diseases Society of America*. Available at https://aidsinfo.nih.gov/contentfiles/lvguidelines/adult_oi.pdf. Accessed October 7, 2016.
27. Sarkar M, Woodland C, Koren G, Einarson ARN (2006) Pregnancy outcome following gestational exposure to azithromycin. *BMC Pregnancy Childbirth* 6:18.
28. Ramsey PS, Vaules MB, Vasdev GM, Andrews WW, Ramin KD (2003) Maternal and transplacental pharmacokinetics of azithromycin. *Am J Obstet Gynecol* 188(3):714–718.
29. Sutton AL, et al. (2015) Perinatal pharmacokinetics of azithromycin for cesarean prophylaxis. *Am J Obstet Gynecol* 212(6):812.e1–812.e6.
30. Jaruratanasirikul S, Hortiwakul R, Tantisarasart T, Phuenpathom N, Tussanasunthornwong S (1996) Distribution of azithromycin into brain tissue, cerebrospinal fluid, and aqueous humor of the eye. *Antimicrob Agents Chemother* 40(3):825–826.
31. Kemp MW, et al. (2014) Maternal intravenous administration of azithromycin results in significant fetal uptake in a sheep model of second trimester pregnancy. *Antimicrob Agents Chemother* 58(11):6581–6591.
32. Stenglein MD, et al. (2014) Ball python nidovirus: A candidate etiologic agent for severe respiratory disease in *Python regius*. *MBio* 5(5):e01484–e14.

MICROBIOLOGY